Organic Light-Emitting Diodes Based on a Columnar Liquid-Crystalline Perylene Emitter

Changmin Keum, David Becker, Emily Archer, Harald Bock, Heinz Kitzerow, Malte Gather, Caroline Murawski

Organic Light-Emitting Diodes Based on a Columnar Liquid-Crystalline Perylene Emitter

*Changmin Keum, David Becker, Emily Archer, Harald Bock, Heinz Kitzerow, Malte C. Gather, and Caroline Murawski**

Liquid crystalline materials possess great potential as emitters in organic light-emitting diodes (OLEDs) due to their self-assembling property, which may lead to anisotropic films and improved charge transport. Here, the key photophysical properties of the columnar liquid crystalline emitter perylene-3,4,9,10-tetracarboxylic tetraethyl ester (PTCTE) are investigated and the material is implemented into OLEDs. It is found that vacuum-deposited PTCTE films exhibit preferential horizontal orientation of the transition dipole moment. Embedding the emitter into different host materials leads to increased photoluminescence quantum yield but reduces molecular orientation compared to the neat film. OLEDs containing PTCTE doped into an exciplex-forming co-host achieve very high luminance exceeding 10 000 cd m^{-2} at 5.7 V, which is among the best performances of OLEDs based on columnar liquid crystalline emitters reported so far.

Dr. C. Keum, E. Archer, Prof. M. C. Gather, Dr. C. Murawski
Organic Semiconductor Centre
SUPA
School of Physics and Astronomy
University of St. Andrews
St. Andrews KY16 9SS, UK
E-mail: caroline.murawski@ksi-meinsberg.de
D. Becker, Prof. H. Kitzerow
Department Chemie
Paderborn University
Warburger Straße 100, Paderborn 33098, Germany
Dr. H. Bock
Centre de Recherche Paul Pascal
CNRS & Université de Bordeaux
115, av. Schweitzer, Pessac 33600, France
Prof. M. C. Gather
Centre for Nanobiophotonics
Department of Chemistry
University of Cologne
Greinstr. 4–6, Köln 50939, Germany
Dr. C. Murawski
Kurt-Schwabe-Institut für Mess- und Sensortechnik Meinsberg e.V.
Kurt-Schwabe-Str. 4, Waldheim 04736, Germany

1. Introduction

Organic semiconducting materials have enabled the advent of cost-effective, large-area, lightweight, and flexible optoelectronic devices. Among them, electroluminescent materials are of particular importance in developing organic light-emitting diodes (OLEDs), one of the major technologies for modern display applications and holding great promise for future solid-state lighting. Currently, the main loss mechanism in OLEDs is the efficiency of light extraction. While OLEDs can reach near 100% internal efficiency, light extraction is typically less than 30% efficient. The orientation of the transition dipole moment (TDM) of emitting molecules with respect to the substrate plane is a key factor determining outcoupling efficiency of OLEDs. Specifically, horizontally oriented transition dipole moments in the emission layer can boost the efficiency by reducing coupling to plasmonic and waveguided modes.[1,2] In the past ten years, several research groups have found that some emitting molecules exhibit a preferential TDM orientation in a host matrix depending on the molecular shape as well as intermolecular and substrate interactions.[3–9] This has been reviewed in refs. [10,11]. Although attempts to further induce horizontal TDM orientation in solid films externally have been reported,[12,13] controlling the TDM orientation of emitters precisely down to the molecular level is extremely challenging, especially when the organic films are deposited via thermal evaporation.

In this regard, organic semiconductors showing liquid crystalline behavior have been of great interest as functional layers in electronic and photonic devices due to their self-assembling properties.[14–18] Discotic liquid crystals (DLC), a class of liquid crystals typically composed of a disc-shaped aromatic core and flexible peripheral chains, can self-organize into columnar phases with strong π–π interactions between discotic cores, which leads to high charge carrier mobility along the axis of the columnar aggregates.[19,20] By taking advantage of these unique electronic and structural features, various types of DLCs have been designed and synthesized to exploit in optoelectronic devices including OLEDs.[21–23]

Perylene derivatives are DLC compounds that typically form flat crystalline structures with tight packing, which often results in formation of excimers. In addition, they exhibit excellent thermal and photochemical stability as well as electron

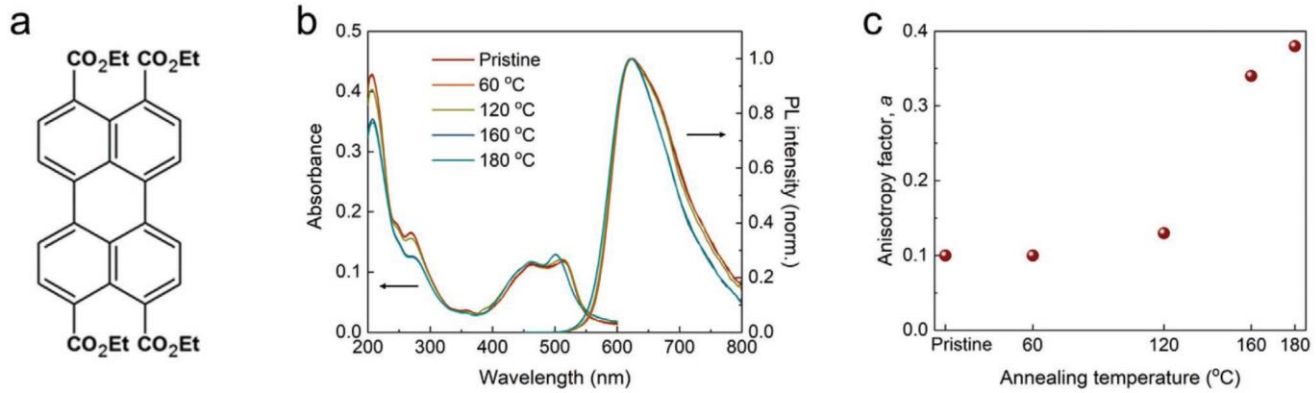

Figure 1. a) Chemical structure of PTCTE. b) Absorbance and normalized PL spectra (λ_{exc} = 300 nm) of PTCTE thin films (nominal thickness, 50 nm) annealed at different temperatures. "Pristine" indicates non-annealed films. c) Anisotropy factor of PTCTE neat films for different annealing temperatures.

transporting and fluorescent emission properties, which make them highly promising as emitters in OLEDs.[24–26] The use of perylene derivatives in OLEDs has been explored by several groups, however, most studies primarily focused on physicochemical properties of materials and their potential applications rather than device performance and characteristics. Hence, emitters were only incorporated in simple OLED structures which often required drive voltages >8 V and achieved a maximum luminance of mostly <1000 cd m^{-2} at voltages higher than 10 V,[27–31] similar to other studies of liquid crystal-based OLEDs.[17,32–35] In order to develop more efficient liquid crystalline OLEDs, the knowledge about the self-assembling properties of DLCs that the community has acquired over the past decades needs to be appropriately integrated with state-of-the-art OLED structures and with the functional materials used in these.

In this publication, we present several different OLED device structures that are based on the DLC emitter perylene-3,4,9,10-tetracarboxylic tetraethyl ester (PTCTE) (**Figure 1**a). PTCTE shows a crystalline phase with columnar structure at room temperature. Furthermore, ordering of PTCTE films can be improved by thermal annealing. Although detailed studies of the compound in both solution and thin film were made previously, key photophysical quantities such as photoluminescence quantum yield (PLQY) and TDM anisotropy remain unknown.[22,29,36,37] Here, we investigate the photophysical properties of PTCTE thin films by measurements of PLQY, TDM orientation, and emission behavior upon annealing. In order to improve PLQY and OLED efficiency, we then incorporated the emitter into different host materials and implemented the host-guest-films into state-of-the-art OLED structures. Using doped charge transport layers and an exciplex-forming co-host structure, we achieved orange fluorescent OLEDs with steep j–V characteristics, onset voltages of 2.7 V, and luminance exceeding 10 000 cd m^{-2} at 5.7 V.

2. Results and Discussion

2.1. Photophysical Properties of PTCTE

In order to assess the potential of PTCTE as emitter material for OLEDs, we first investigated absorbance, photoluminescence (PL) spectra, PLQY, and TDM anisotropy of plain 50 nm thick PTCTE films. While PTCTE films may be fabricated from both solution and vacuum thermal evaporation,[22] having the interface between the organic surface and the vacuum is generally beneficial to achieve anisotropic TDM orientation in thin organic films.[6] Thus, we thermally evaporated all materials in this study. The absorption showed a strong band with peaks at 464 and 515 nm (Figure 1b), which was red-shifted compared to the absorption in solution (400–480 nm).[22] The PL showed a broad featureless spectrum peaking at 624 nm and with 126 nm full-width at half maximum (FWHM), which originated from formation of excimers.[37]

Due to the columnar liquid crystalline structure of PTCTE, we expected a preferred orientation of the molecule on the substrate. Measurement of TDM orientation via angle-resolved p-polarized PL spectra fitted to a transfer matrix model as described in literature[1–3,6,9] revealed a preferential horizontal orientation of the transition dipoles with an anisotropy of a = 0.1 (a denotes the ratio of vertical dipoles over all dipoles; a = 0 for complete horizontal orientation and a = 0.33 for isotropic orientation; Figure 1c; Figure S1, Supporting Information). Since annealing of liquid crystalline materials may lead to denser packing and improved structural order,[29] we also studied the TDM orientation for heated films. For annealing temperatures up to 120 °C only minor changes were observed, but annealing to 160 °C and above caused slight narrowing of the PL spectra and molecular re-orientation (Figure 1b,c). This is in agreement with previously measured phase transitions at 134 and 150 °C.[37] Thus, the preferential horizontal TDM orientation obtained at room temperature vanished upon annealing and transition dipoles became isotropically oriented, as previously observed also for other molecules.[38,39] The PLQY of the as-deposited film was 13.1%.

2.2. Simple OLEDs with PTCTE Emitter

We incorporated PTCTE as neat emission layer (EML) and electron transport layer (ETL) into simple bi-layer OLEDs using either 2,2′,7,7′-tetrakis(*N*,*N*′-di-p-methylphenylamino)-9,9′-spirobifluorene (Spiro-TTB) or *N*,*N*′-di(naphtalene-1-yl)-*N*,*N*′-diphenylbenzidine (NPB) as hole transport layer (HTL) and LiF/Al as cathode (**Figure 2**a). This structure served as a reference to compare to literature devices using similar

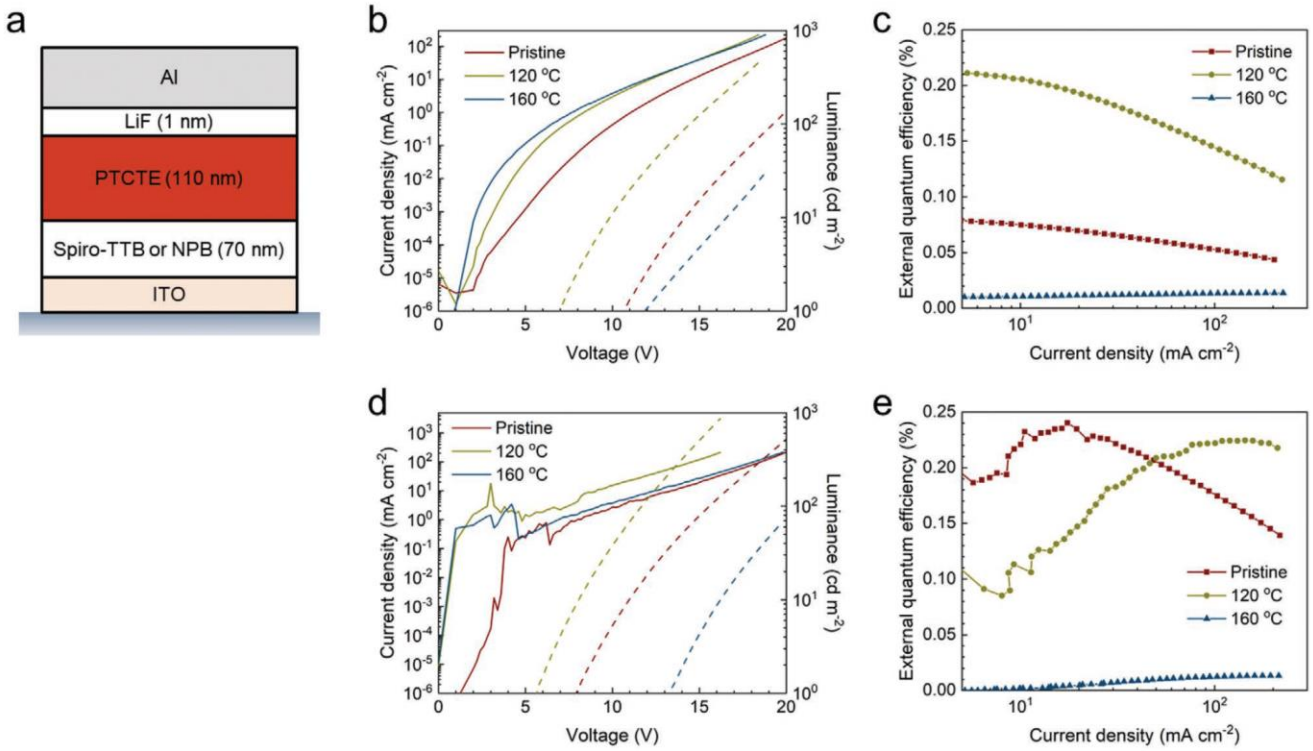

Figure 2. a) Simplified DLC OLED structure with undoped layers. b,d) Current density (solid lines) and luminance (dashed lines) versus voltage characteristics and c,e) external quantum efficiency as a function of current density for DLC OLEDs with Spiro-TTB (b,c) and NPB HTL (d,e) before and after annealing at different temperatures.

bi-layer structures.[22,27,28] We used four different PTCTE thicknesses ranging from 50 to 110 nm. The complete OLED characteristics are shown in Figure S2, Supporting Information. With increasing PTCTE thickness, the external quantum efficiency (EQE) increased for both HTLs. At the same time, the current density strongly decreased due to the low charge carrier mobility of PTCTE, which was previously estimated to 1–10 × 10^{-8} cm^2 V^{-1} s^{-1}.[29] Spiro-TTB as HTL led to lower leakage currents than NPB and, thus, more stable operation at low voltages, however, resulted in three times lower efficiency (Figure 2; Figure S2, Supporting Information). We believe that especially the Spiro-TTB devices suffered from charge imbalance created by an excess of electrons. This is evidenced by: 1) the observed increase in EQE for thicker PTCTE films, which reduced electron transport, and 2) by the higher EQE observed for NPB compared to Spiro-TTB, where the latter presented a larger energy barrier for hole injection into PTCTE (cf. energy levels in Figure S4b, Supporting Information).

Figure 2b,c shows the *j*–*V*–*L* characteristics and EQE of the best Spiro-TTB device. A luminance of 181 cd m^{-2} was reached at 20 V, similar to previous results,[22,27,28] and the EQE showed a maximum of 0.08%. Upon annealing of the device to 120 °C, we observed an increase in charge transport, especially at lower voltages. This may be due to enhanced structural order at the interface between ITO and Spiro-TTB, which led to improved hole injection. As argued above, the non-annealed devices suffered from charge imbalance due to hole deficiency. Thus, heating of the devices could balance charge injection, which then also improved the EQE reaching now up to 0.21%. Further annealing to 160 °C caused a strong drop in EQE, probably caused by reorganization of the Spiro-TTB HTL (glass transition temperature, T_g = 146 °C).[40] As shown in Figure 2d,e, annealing of samples with NPB HTL did not lead to significant improvement but instead caused very instable operation due to the low T_g of NPB being only 95 °C.[41] The electroluminescence (EL) spectra of the OLEDs peak at 610 nm, indicating that emission originates predominantly from excimers (Figure S2c, Supporting Information).[22,37] The spectra are nearly independent of HTL material and PTCTE thickness, suggesting that optical effects play only a minor role.

2.3. Photophysical Properties of PTCTE Doped into Different Host Materials

The low PLQY of PTCTE of only 13% is probably caused by its dense molecular packing, which leads to excimer formation and contributes to concentration quenching. In order to improve the PLQY, we embedded the liquid crystalline emitter into different host materials. Chemical structures of selected hosts (NPB, 4,4′,4″-tris(*N*-carbazolyl)-triphenylamine (TCTA), 4,6-bis(3,5-di(pyridin-3-yl)phenyl)-2-methylpyrimidine (B3PYMPM), and 2,2′,2″-(1,3,5-benzinetriyl)tris(1-phenyl-1-H-benzimidazole) (TPBi)) are shown in Figure 3a. NPB and TCTA are hole-transporting materials while B3PYMPM and TPBi predominantly transport electrons. As a result, the PLQY was reduced when doping PTCTE at 2 wt% in NPB and TCTA hosts but increased to up to 56% using TPBi as host (**Table 1**).

The PL spectra of PTCTE doped films are shown in **Figure 3**b. Doping the emitter into NPB led to a slight red-shift

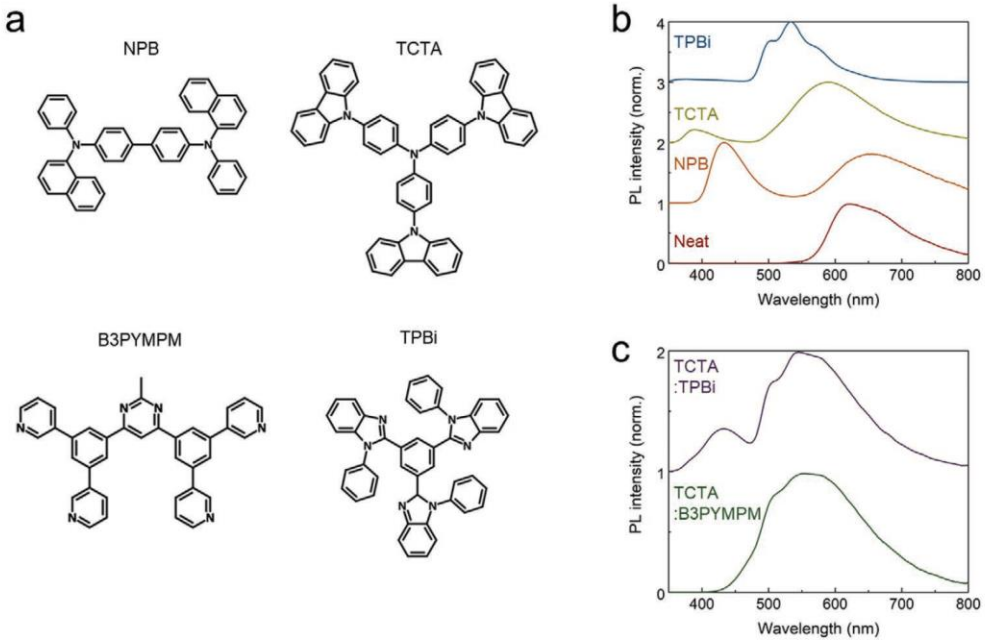

Figure 3. a) Chemical structure of the host materials. b) Normalized PL spectra (λ_{exc} = 300 nm) of PTCTE in different hosts. c) Same for PTCTE doped into co-host systems.

of the excimer peak to 649 nm and the formation of an additional strong peak at 433 nm, which originated from NPB emission. This indicates strong phase separation in NPB and may be the origin of the observed low PLQY in this system. Embedding the emitter into the other host materials instead caused a blue-shift of the spectrum. Using TCTA as a host, the emission peaked at 590 nm and was similarly featureless as in NPB. Thus, excimer emission appeared to be dominant in this film as well. Additionally, emission from the TCTA host is detected at ≈390 nm.[42] However, when doping the emitter into TPBi the spectrum showed a peak at 533 nm with clear vibronic progression while the excimer emission of PTCTE vanished. The high PLQY observed for TPBi:PTCTE films (56%) thus originates from pure singlet emission and indicates that emitter molecules are well dispersed within the film.

The orientation of the transition dipoles of neat PTCTE films became less horizontal when the emitter was embedded in TPBi and TCTA, with a = 0.22 and 0.26, respectively (Table 1; Figure S3a, Supporting Information). With an NPB host, purely isotropic orientation was observed, which may be related to its lower T_g compared to TCTA (151 °C) and TPBi (122 °C).[43] Furthermore, PTCTE molecules showed a more preferential horizontal orientation when embedded in TPBi, which is composed of a more rigid core compared to TCTA.

Additionally, we tested exciplex-forming co-host structures of TCTA:B3PYMPM and TCTA:TPBi. Exciplex-forming co-hosts have previously contributed to preferential TDM orientation and may furthermore improve charge balance and reduce driving voltages in OLEDs.[2,42,44] In our case, however, embedding PTCTE into co-hosts caused neither an improvement in PLQY nor in TDM orientation (Table 1; Figure S3b, Supporting Information). The PL spectra of PTCTE in TCTA:TPBi co-host showed both singlet PTCTE emission as well as excimer emission (Figure 3c). Furthermore, host exciplex emission appeared at ≈440 nm.[44] Emission from the TCTA:B3PYMPM co-host system showed a similar spectrum, however, the PTCTE singlet may have been overlapped by host exciplex emission at ≈490 nm.[42] Thus, the co-host systems suggest that still larger domains of PTCTE were present in those films, which also correlates with the rather low PLQY obtained.

In conclusion, TPBi seems most promising as host for well-dispersed PTCTE films. Although the strong horizontal TDM orientation observed in neat PTCTE films is reduced in TPBi, this host still provides significant TDM anisotropy and additionally strongly improves PLQY. This may be due to the more polar character of TPBi,[45] which is similar to the polar ester groups in PTCTE and thus possibly prevents the formation of clustered emitter domains.

Table 1. PLQY (λ_{exc} = 298 nm) and anisotropy factor a of neat PTCTE films and PTCTE doped into different host materials at 2 wt%.

Host	Neat	NPB	TCTA	TPBi	TCTA:B3PYMPM	TCTA:TPBi
PLQY [%]	13.1	2.6	11.5	56.4	13.2	13.6
Anisotropy factor, a	0.10	0.33	0.26	0.22	0.32	0.28

2.4. Embedding PTCTE into State-of-the-Art OLEDs

Next, we embedded PTCTE into EMLs either as neat emitter or doped at 2 wt% into the host materials studied above and incorporated this EML into state-of-the-art OLED structures (**Table 2**, **Figure 4**a). Compared to using PTCTE as neat emitter, embedding it into hosts may lead to three different effects, namely, changes in charge transport, radiative efficiency, and outcoupling efficiency. While the outcoupling efficiency will slightly decrease due to the reduced TDM

Table 2. Electron blocking layer (EBL), EML, and hole blocking layer (HBL) materials used for devices with doped charge transport layers (Figure 4a). The EML was doped with 2 wt% PTCTE (except for neat layer of PTCTE, device D1).

Device	EBL	EML	HBL
D1	NPB	Neat (PTCTE)	BAlq
D2	NPB	NPB	BAlq
D3	NPB	TCTA	BAlq
D4	NPB	TPBi	TPBi
D5[a)]	NPB	TCTA:TPBi	TPBi
D6	NPB	TCTA:B3PYMPM	B3PYMPM

[a)]This device contained a Spiro-TTB:F6-TCNNQ HTL with a thickness of 50 nm.

orientation in host–guest systems, we expect significant gain in charge transport. Additionally, in the case of TPBi as the host, the increased PLQY will lead to a strong improvement in radiative efficiency.

In order to reduce resistive losses and facilitate Ohmic charge carrier injection, the devices used doped charge transport layers (so-called p-i-n structure).[46,47] Figure 4b,e shows the current–voltage–luminance characteristics. Compared to the simple OLED structure (Figure 2), current transport and luminance increased tremendously for all host–guest systems. However, the device containing PTCTE as neat emitter (D1) was only very weakly emissive, despite showing the largest current transport.

Embedding PTCTE into a matrix resulted instead in strongly increased luminance, which reached values exceeding 1000 cd m^{-2} at 5.3 V for NPB and TCTA hosts. For these two host materials, we also tested TCTA instead of NPB as electron blocking layer (EBL) but leakage currents significantly increased and current transport became massively hindered due to the energy barrier between Spiro-TTB and TCTA (Figure S4a,b, Supporting Information). The TPBi host with its very deep HOMO level introduced an additional energy barrier for hole injection that led to reduced charge transport, as observed by the s-kink in *j–V* characteristics. We suggest that the first increase in *j–V* between 3 and 5 V in this device is related to successful electron injection into TPBi. Hole injection into the EML, however, was massively hindered due to the large energy difference in the HOMO levels of NPB and TPBi (see energy level diagram in Figure S5, Supporting Information). Instead, the similar LUMO energies of NPB and TPBi (–2.7 eV) enabled a pathway for electrons to leak through the device without recombination. Thus, light was only emitted after successful hole injection into the EML (from 4.8 V upward). Compared to the single host systems, *j–V* characteristics further improved in the co-host systems as expected for exciplex-forming co-hosts due to their reduced energy gaps for electron and hole injection into the EML. Here, a luminance of 1000 cd m^{-2} was achieved at only 4.1 V for both TCTA:B3PYMPM and TCTA:TPBi co-hosts.

The EQE of the single host systems was highest when using TPBi and reached a maximum EQE of 0.45%. However, compared to the high PLQY of 56.4% in this host, the low EQE indicates significant internal losses, probably caused by the large hole injection barrier, which likely led to charge carrier imbalance. An improvement in EQE is observed for OLEDs based on the co-host system of TCTA:TPBi, which reached a maximum EQE of 0.78%. Given the relatively low PLQY of this system of only 13.2% (Table 1), the achieved EQE is already close to the estimated maximum value of 0.83%, which would be possible in this system considering that a fluorescent emitter was used (resulting in a spin factor of 0.25) and assuming a maximum outcoupling efficiency of around 25%.

For most host–guest systems and for the neat emitter, the EL spectra were slightly blue-shifted compared to their respective PL spectra (Figure 4d,g). Furthermore, the higher energy host singlet and exciplex emission observed in PL from single and co-hosts, respectively, are significantly reduced in EL. This

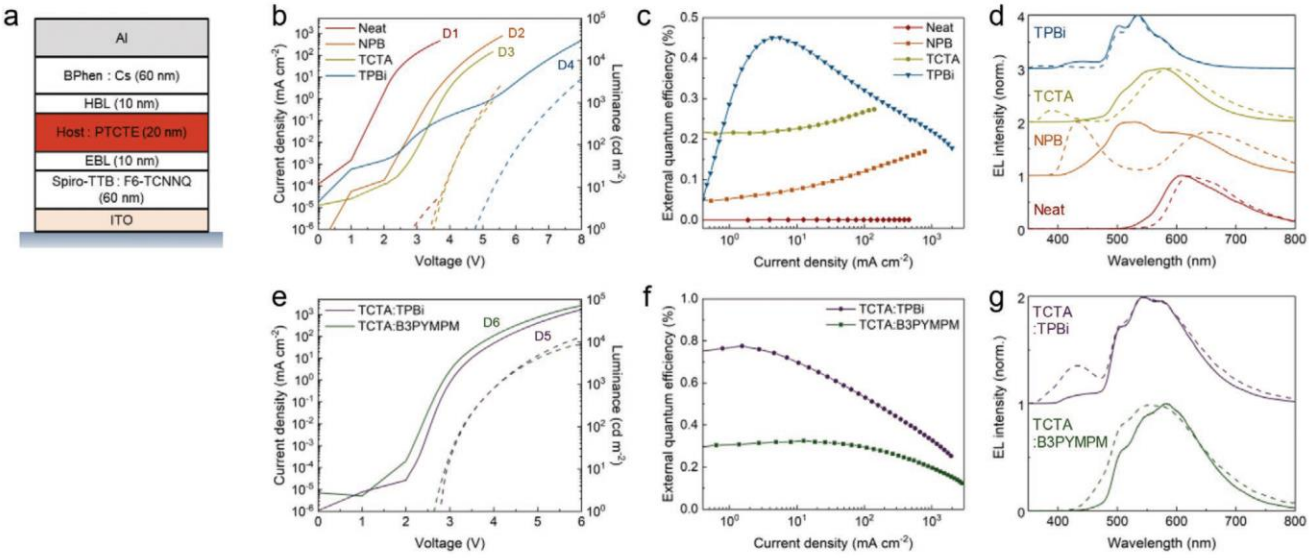

Figure 4. a) Layer structure of p-i-n type DLC OLED stacks. b,e) Current density (solid lines) and luminance (dashed lines) as a function of the voltage (D1-6 indicate the respective OLEDs defined in Table 2), c,f) external quantum efficiency, and d,g) normalized EL spectra recorded at 4 V for PTCTE-based p-i-n OLEDs fabricated with different host materials (top row: single host; bottom row: co-host system). Dashed lines in (d) and (g) show the corresponding PL spectra from Figure 3b,c for comparison.

may be caused by direct formation of excitons on the guest. For the NPB host, the EL spectrum changed dramatically from pure PTCTE excimer and NPB singlet emission in the case of PL to nearly white emission in EL (CIE coordinates: x,y = (0.373,0.452), peak: 528 nm, FWHM: 200 nm). Here, the spectral shape indicates emission from both PTCTE excimer and singlet states. When fabricating OLEDs, the organic layers present underneath the EML possibly reduced molecular clustering of emitter molecules while in PL samples the underlying glass substrate caused stronger formation of PTCTE domains. Furthermore, the spectrum strongly blue-shifted with applied voltage, which suggests that the higher energetic singlet emission only became efficient at higher drive voltages while excimer emission was dominating at low voltages (Figure S4c,d, Supporting Information).

3. Conclusions

In summary, we studied the PL and EL properties of the liquid crystalline emitter PTCTE. The emitter showed preferential horizontal orientation of its TDM, pure excimer emission, and relatively low PLQY. Doping PTCTE into different host materials, the PLQY was increased and emission from the singlet state was observed due to suppressed molecular clustering. Our data further suggest that efficient suppression of excimer emission is important to obtain high PLQY. We then embedded PTCTE host–guest systems in state-of-the-art OLED stacks, which significantly improved efficiency, that is, electrical efficiency and radiative decay, compared to simple bi-layer OLEDs that contained the emitter as neat EML. **Figure 5** summarizes the maximum EQE, luminous efficacy (LE), and current efficiency (CE) of the investigated devices. Using a co-host of TCTA:TPBi, we achieved maximum efficiencies of 0.8% EQE, 2.2 lm W^{-1}, and 2.1 cd A^{-1}. Future studies should focus on improving OLED performance using TPBi as host, for which we observed highest PLQY and strongest TDM anisotropy of all host materials studied. For OLEDs incorporating a TPBi host, other EBL materials should be tested in order to improve hole injection into the EML. This would optimize charge balance and may lead to EQE values of up to 4.2% assuming a light outcoupling efficiency in line with the TDM anisotropy of this system (i.e., about 30%). With the broad emission spectrum observed, we believe that this emitter holds also great potential for creating simple white OLEDs with high color rendering, even without using additional emitters as suggested in ref. [27].

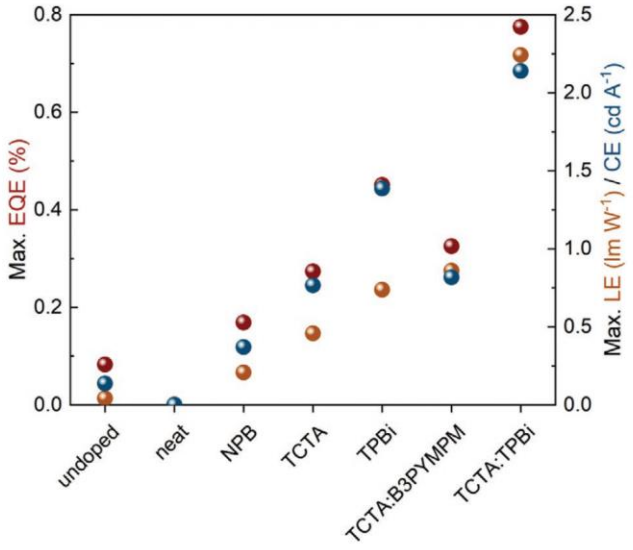

Figure 5. Summary of maximum EQE, LE, and CE of the DLC OLEDs investigated in this study. "Undoped" refers to the simple device (Figure 2a) with Spiro-TTB HTL and 110 nm PTCTE. All other devices refer to the p-i-n stack with variation of EML materials (Figure 4a).

4. Experimental Section

All samples were fabricated by thermal evaporation in a high vacuum chamber (Angstrom EvoVac) at a base pressure of 10^{-7} mbar. For photophysical measurements, 50 nm films were fabricated either on glass (orientation measurements), quartz (for measurement of absorbance, PL spectra, and PLQY), or silicon substrates (measurement of n and k values). Glass samples were encapsulated to minimize degradation during PL measurements. Emission spectra were measured in a fluorimeter (Edinburgh Instruments FLS1000) and averaged over 10 points (20 nm). Absorbance was measured in a spectrophotometer (Cary 300). PLQY was recorded in an integrating sphere (Hamamatsu C9920) in nitrogen environment. The TDM orientation was measured in a custom-built goniometer as described elsewhere.[3] Briefly, samples were mounted on a rotary stage and coupled to an index-matched semi-cylindrical glass lens. Upon excitation with a UV LED at 365 nm, the transverse magnetic component of the sample emission was recorded using a polarizer and a fiber-coupled spectrometer (OceanOptics Maya LSL). The TDM orientation was then calculated by fitting the measured spectra to the spectral radiant intensity (SRI) $I(\theta,\lambda)$ obtained by transfer-matrix simulations: $I(\theta, \lambda) = a \times I_{TM,v}(\theta, \lambda) + (1 - a) \times I_{TM,h}(\theta, \lambda)$. Here, $I_{TM,v}/I_{TM,h}$ describes the transverse magnetic components of the SRI emitted vertically/horizontally to the substrate plane, θ is the collection angle relative to the substrate plane, and λ is the wavelength. For this, the complex refractive indices of all studied films were determined by ellipsometry (J.A. Woollam Co., M-2000DI).

OLEDs were fabricated on cleaned glass substrates coated with 90 nm pre-patterned ITO (Thin Film Devices, Inc.). Samples were encapsulated in nitrogen atmosphere directly after fabrication with getter-embedded glass lids. The following materials were used: Spiro-TTB as HTL; 2,2′-(perfluoronaphthalene-2,6-diylidene)dimalononitrile (F6-TCNNQ) as p-dopant at 4 wt%; NPB as HTL, EBL, and host; TCTA as EBL and host; TPBi as host and HBL; B3PYMPM as host and HBL; bis-(2-methyl-8-chinolinolato)-(4-phenyl-phenolato)-aluminum(III) (BAlq) as HBL; 4,7-diphenyl-1,10-phenanthroline (BPhen) n-doped with Cs at 2 wt% as ETL; lithium fluoride (LiF) as electron injection layer in simple bi-layer OLEDs; 100 nm aluminum as cathode.

The device characteristics were recorded with a source-measure unit (Keithley 2400) and a calibrated silicon photodiode. EL spectra were measured with a spectrograph (Oriel MS125) coupled to a CCD camera (Andor DV420-BU). Efficiencies were calculated assuming Lambertian emission. For annealing experiments, samples were placed on a hotplate for 3 min and measured after cooling down to room temperature.

Supporting Information

Supporting Information is available from the Wiley Online Library or from the author. The research data supporting this publication can be accessed at https://doi.org/10.17630/c0262859-1d55-4463-9e4f-883859a7ac8f.

Acknowledgements

This research was financially supported by the EPSRC NSF-CBET lead agency agreement (EP/R010595/1, 1706207). C.K. acknowledges support from the Basic Science Research Program through the National Research Foundation of Korea (NRF) funded by the Ministry of Education (2017R1A6A3A03012331). Diese Arbeit wurde mitfinanziert durch Steuermittel auf der Grundlage des vom Sächsischen Landtag beschlossenen Haushaltes.

Conflict of Interest

The authors declare no conflict of interest.

Keywords

discotic liquid crystals, high brightness, organic light-emitting diodes, perylene, transition dipole moment orientation

[1] J. Frischeisen, D. Yokoyama, A. Endo, C. Adachi, W. Brütting, *Org. Electron.* **2011**, *12*, 809.
[2] K.-H. Kim, S. Lee, C.-K. Moon, S.-Y. Kim, Y.-S. Park, J.-H. Lee, J. W. Lee, J. Huh, Y. You, J.-J. Kim, *Nat. Commun.* **2014**, *5*, 4769.
[3] J. Frischeisen, D. Yokoyama, C. Adachi, W. Brütting, *Appl. Phys. Lett.* **2010**, *96*, 073302.
[4] P. Liehm, C. Murawski, M. Furno, B. Lüssem, K. Leo, M. C. Gather, *Appl. Phys. Lett.* **2012**, *101*, 253304.
[5] A. Graf, P. Liehm, C. Murawski, S. Hofmann, K. Leo, M. C. Gather, *J. Mater. Chem. C* **2014**, *2*, 10298.
[6] M. J. Jurow, C. Mayr, T. D. Schmidt, T. Lampe, P. I. Djurovich, W. Brütting, M. E. Thompson, *Nat. Mater.* **2016**, *15*, 85.
[7] C. Moon, K.-H. Kim, J.-J. Kim, *Nat. Commun.* **2017**, *8*, 791.
[8] C. Murawski, C. Elschner, S. Lenk, S. Reineke, M. C. Gather, *Org. Electron.* **2018**, *53*, 198.
[9] J. Kim, T. Batagoda, J. Lee, D. Sylvinson, K. Ding, P. G. Saris, U. Kaipa, I. W. H. Oswald, M. A. Omary, M. E. Thompson, S. R. Forrest, *Adv. Mater.* **2019**, *31*, 1900921.
[10] T. D. Schmidt, T. Lampe, M. R. D. Sylvinson, P. I. Djurovich, M. E. Thompson, W. Brütting, *Phys. Rev. Appl.* **2017**, *8*, 037001.
[11] K.-H. Kim, J. Kim, *Adv. Mater.* **2018**, *30*, 1705600.
[12] T. Arai, K. Goushi, H. Nomura, T. Edura, C. Adachi, *Appl. Phys. Lett.* **2011**, *99*, 053303.
[13] C.-M. Keum, S. Liu, A. Al-Shadeedi, V. Kaphle, M. K. Callens, L. Han, K. Neyts, H. Zhao, M. C. Gather, S. D. Bunge, R. J. Twieg, A. Jakli, B. Lüssem, *Sci. Rep.* **2018**, *8*, 699.
[14] G. Lüssem, J. H. Wendorff, *Polym. Adv. Technol.* **1998**, *9*, 443.
[15] M. O'Neill, S. M. Kelly, *Adv. Mater.* **2003**, *15*, 1135.
[16] K. S. Whitehead, M. Grell, D. D. C. Bradley, M. Jandke, P. Strohriegl, *Appl. Phys. Lett.* **2000**, *76*, 2946.
[17] M. P. Aldred, A. E. A. Contoret, S. R. Farrar, S. M. Kelly, D. Mathieson, M. O'Neill, W. C. Tsoi, P. Vlachos, *Adv. Mater.* **2005**, *17*, 1368.
[18] M. Funahashi, F. Zhang, N. Tamaoki, *Adv. Mater.* **2007**, *19*, 353.
[19] B. R. Kaafarani, *Chem. Mater.* **2011**, *23*, 378.
[20] C. Zou, J. Wang, M. Wang, Y. Wu, K. Gu, Z. Shen, G. Xiong, H. Yang, L. Jiang, T. Ikeda, *Small* **2018**, *14*, 1800557.
[21] S. K. Pathak, R. K. Gupta, S. Nath, D. S. S. Rao, S. K. Prasad, A. S. Achalkumar, *J. Mater. Chem. C* **2015**, *3*, 2940.
[22] J. Vollbrecht, C. Wiebeler, A. Neuba, H. Bock, S. Schumacher, H. Kitzerow, *J. Phys. Chem. C* **2016**, *120*, 7839.
[23] J. De, S. P. Gupta, S. S. Swayamprabha, D. K. Dubey, I. Bala, I. Sarkar, G. Dey, J.-H. Jou, S. Ghosh, S. K. Pal, *J. Phys. Chem. C* **2018**, *122*, 23659.
[24] F. Würthner, *Chem. Commun.* **2004**, *4*, 1564.
[25] S. K. Gupta, S. Setia, S. Sidiq, M. Gupta, S. Kumar, S. K. Pal, *RSC Adv.* **2013**, *3*, 12060.
[26] R. K. Gupta, A. A. Sudhakar, *Langmuir* **2019**, *35*, 2455.
[27] T. Hassheider, S. A. Benning, H.-S. Kitzerow, M.-F. Achard, H. Bock, *Angew. Chem., Int. Ed.* **2001**, *40*, 2060.
[28] I. Seguy, P. Destruel, H. Bock, *Synth. Met.* **2000**, *111-112*, 15.
[29] J. Vollbrecht, S. Blazy, P. Dierks, S. Peurifoy, H. Bock, H. Kitzerow, *ChemPhysChem* **2017**, *18*, 2024.
[30] J. Eccher, A. C. B. Almeida, T. Cazati, H. von Seggern, H. Bock, I. H. Bechtold, *J. Lumin.* **2016**, *180*, 31.
[31] R. K. Gupta, D. Das, M. Gupta, S. K. Pal, P. K. Iyer, A. S. Achalkumar, *J. Mater. Chem. C* **2017**, *5*, 1767.
[32] A. Liedtke, M. O'Neill, A. Wertmöller, S. P. Kitney, S. M. Kelly, *Chem. Mater.* **2008**, *20*, 3579.
[33] A. K. Yadav, B. Pradhan, H. Ulla, S. Nath, J. De, S. K. Pal, M. N. Satyanarayan, A. S. Achalkumar, *J. Mater. Chem. C* **2017**, *5*, 9345.
[34] I. Bala, L. Ming, R. A. K. Yadav, J. De, D. K. Dubey, S. Kumar, H. Singh, J.-H. Jou, K. Kailasam, S. K. Pal, *ChemistrySelect* **2018**, *3*, 7771.
[35] J. De, W. Y. Yang, I. Bala, S. P. Gupta, R. A. K. Yadav, D. K. Dubey, A. Chowdhury, J. H. Jou, S. K. Pal, *ACS Appl. Mater. Interfaces* **2019**, *11*, 8291.
[36] J. Vollbrecht, O. Kasdorf, V. Quiring, H. Suche, H. Bock, H.-S. Kitzerow, *Appl. Phys. Lett.* **2013**, *103*, 043303.
[37] S. A. Benning, T. Haßheider, S. Keuker-Baumann, H. Bock, F. D. Sala, T. Frauenheim, H. Kitzerow, *Liq. Cryst.* **2001**, *28*, 1105.
[38] T. Komino, H. Tanaka, C. Adachi, *Chem. Mater.* **2014**, *26*, 3665.
[39] S. S. Dalal, D. M. Walters, I. Lyubimov, J. J. de Pablo, M. D. Ediger, *Proc. Natl. Acad. Sci. USA* **2015**, *112*, 4227.
[40] T. P. I. Saragi, T. Fuhrmann-Lieker, J. Salbeck, *Adv. Funct. Mater.* **2006**, *16*, 966.
[41] S. A. van Slyke, C. H. Chen, C. W. Tang, *Appl. Phys. Lett.* **1996**, *69*, 2160.
[42] Y.-S. Park, S. Lee, K.-H. Kim, S.-Y. Kim, J.-H. Lee, J.-J. Kim, *Adv. Funct. Mater.* **2013**, *23*, 4914.
[43] C. Mayr, W. Brütting, *Chem. Mater.* **2015**, *27*, 2759.
[44] X. Wang, R. Wang, D. Zhou, J. Yu, *Synth. Met.* **2016**, *214*, 50.
[45] S.-R. Park, D. H. Shin, S.-M. Park, M. C. Suh, *RSC Adv.* **2017**, *7*, 28520.
[46] K. Walzer, B. Maennig, M. Pfeiffer, K. Leo, *Chem. Rev.* **2007**, *107*, 1233.
[47] B. Lüssem, M. Riede, K. Leo, *Phys. Status Solidi A* **2013**, *210*, 9.